Future Possibilities of Atmospheric Neutrino Measurements

Masato SHIOZAWA
Institute for Cosmic Ray Research, University of Tokyo, Higashi-Mozumi, Kamioka-cho, Hida City, Gifu 506-1205, Japan
Takaaki KAJITA
Institute for Cosmic Ray Research, University of Tokyo, 5-1-5 Kashiwa-no-Ha, Kashiwa City, Chiba 277-8582, Japan
Shoei NAKAYAMA
Institute for Cosmic Ray Research, University of Tokyo, 5-1-5 Kashiwa-no-Ha, Kashiwa City, Chiba 277-8582, Japan
Yoshihisa OBAYASHI
Institute for Cosmic Ray Research, University of Tokyo, Higashi-Mozumi, Kamioka-cho, Hida City, Gifu 506-1205, Japan
Kimihiro OKUMURA
Institute for Cosmic Ray Research, University of Tokyo, 5-1-5 Kashiwa-no-Ha, Kashiwa City, Chiba 277-8582, Japan

Abstract

While neutrino flavor mixing has been established by atmospheric neutrino experiments and solar/reactor neutrino experiments, there are still remaining mixing parameters and CP phase to be explored. In this article, sensitivities for measuring these parameters by future atmospheric neutrino experiments are discussed assuming the same set of systematic uncertainties and the same detector performance of Super-Kamiokande. It was found that there is possibility to discriminate the octants of θ_{23}. Moreover, if θ_{13} is close to current reactor limit, there is a good opportunity to confirm nonzero θ_{13} and even measure CP phase in lepton sector.

1. Introduction

Neutrino mixing matrix U, that translates neutrino mass eigenstates into flavor eigenstates $(\nu_e, \nu_\mu, \nu_\tau)^T = U(\nu_1, \nu_2, \nu_3)^T$, is called as Maki-Nakagawa-Sakata

pp. 57–67

(MNS) matrix and is expressed as;

$$\begin{aligned} U &= \begin{pmatrix} U_{e1} & U_{e2} & U_{e3} \\ U_{\mu 1} & U_{\mu 2} & U_{\mu 3} \\ U_{\tau 1} & U_{\tau 2} & U_{\tau 3} \end{pmatrix} \\ &= \begin{pmatrix} 1 & 0 & 0 \\ 0 & c_{23} & s_{23} \\ 0 & -s_{23} & c_{23} \end{pmatrix} \begin{pmatrix} c_{13} & 0 & s_{13}e^{i\delta} \\ 0 & 1 & 0 \\ -s_{13}e^{-i\delta} & 0 & c_{13} \end{pmatrix} \begin{pmatrix} c_{12} & s_{12} & 0 \\ -s_{12} & c_{12} & 0 \\ 0 & 0 & 1 \end{pmatrix} \end{aligned} \quad (1)$$

where c_{ij} and s_{ij} represent sinθ_{ij} and cosθ_{ij}, respectively. Among 4 parameters, θ_{23} has been discovered and measured as $\sim \pi/4$ by atmospheric neutrino observations assuming pure $\nu_\mu \to \nu_\tau$ 2 flavor oscillation scheme [1, 2]. Because 2 flavor oscillation probability is a function of $\sin^2 2\theta_{23}$, both θ_{23} and $\pi/2 - \theta_{23}$ give same probability. This degeneracy is resolved in full 3 flavor oscillation scheme. It is a important topic to discriminate the θ_{23} octants by future atmospheric neutrino experiments. On the other hand, θ_{12} has been measured as $\sin^2 2\theta_{12} \sim 0.825$ by solar and reactor neutrino experiments [3]. However, nonzero θ_{13} has not been measured and only an upper limit of $s_{13}^2 < 0.04$ was obtained so far [4]. Moreover, CP phase δ is experimentally not known at all.

To explore these parameters is one of most important subjects in elementary particle physics and possibility to measure these parameters by atmospheric neutrino experiments is discussed in this article.

2. Oscillation Probability

Oscillation probabilities in the case of 3 flavor neutrino scheme have been discussed by many authors [5]. In sub-GeV energy region, oscillation effect in electron neutrino flux can be analytically calculated [6];

$$\begin{aligned} \frac{\Phi(\nu_e)}{\Phi_0(\nu_e)} - 1 \;\approx\; & P_2(r \cdot c_{23}^2 - 1) \\ & - r \cdot \tilde{s}_{13} \cdot \tilde{c}_{13}^2 \cdot \sin 2\theta_{23}(\cos\delta \cdot R_2 - \sin\delta \cdot I_2) \\ & + 2\tilde{s}_{13}^2(r \cdot s_{23}^2 - 1) \end{aligned} \quad (2)$$

where P_2 is 2 neutrino transition probability of $\nu_e \to \nu_{\mu,\tau}$ in matter which is driven by solar neutrino mass difference (Δm_{12}^2). r is ν_μ/ν_e flux ratio as a function of neutrino energy. Mixing angles with tilde are effective mixing angles in the earth and $\tilde{s}_{13}^2$ could become large at $5 \sim 10$ GeV neutrino energy by matter potential. In order to understand the behavior of these three terms, Figure 1 shows ν_e flux as a function of neutrino energy from numerical calculations of oscillation probabilities

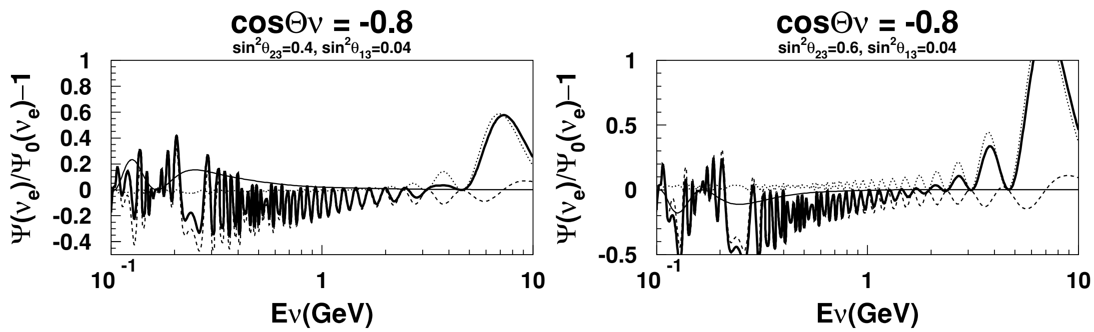

Fig 1. Oscillated ν_e flux relative to the non-oscillated flux as a function of neutrino energy. $s_{23}^2 = 0.4$ (left) and $s_{23}^2 = 0.6$ (right) and other parameters are common as $(\sin^2 2\theta_{12}, s_{23}^2, s_{13}^2, \delta, \Delta m_{12}^2, \Delta m_{23}^2) = (0.825, 0.4 \text{or} 0.6, 0.04, 45°, 8.3 \times 10^{-5}\text{eV}^2, 2.5 \times 10^{-3}\text{eV}^2)$. Zenith angle of neutrino direction is taken to be -0.8. Thin solid lines, dashed lines, and dotted lines correspond to Δm_{12}^2 term, interference term, and θ_{13} resonance term, respectively (see Equation 2). Thick solid lines are total fluxes.

by taking into account the matter density profile in the earth [7]. Thin solid lines correspond to the first term (Δm_{12}^2 term) in Equation 2. This term is visible only in sub-GeV energy region due to the small Δm_{12}^2. Due to the fact that $r \sim 2$ in sub-GeV region, the effect of the Δm_{12}^2 term has different signs (ν_e enhancement or suppression) in the case of the first octant of 2-3 angle ($c_{23}^2 > 0.5$) and the second octant ($c_{23}^2 < 0.5$). Dotted lines correspond to the third term (θ_{13} resonance term) in Equation 2. This term could make a significant contribution in $5 \sim 10$ GeV region if θ_{13} is not very small. Future observations of electron excess in multi-GeV range would enable us to measure nonzero θ_{13}. Moreover, this term has a discrimination power of θ_{23} octant because this term is proportional to $(r \cdot s_{23}^2 - 1)$. Finally, dashed lines in Figure 1 correspond to the second term (interference term) in Equation 2. CP phase effect appears in the region from sub-GeV to multi-GeV neutrino energy. This term is proportional to θ_{13} in matter and there may be possibility to measure CP phase in the case of large θ_{13}.

3. Tools and Assumptions

In this study, atmospheric neutrino interactions are simulated using the flux calculation and interaction models used in the Super-Kamiokande (SK) analyses [2]. Detailed full simulation of a detector and event reconstructions are performed by the SK detector simulator and the standard reconstruction tools [2]. We have obtained Monte Carlo (MC) events which statistics correspond to 100 year exposure of SK.

Oscillation probabilities are calculated by taking into account the full parameters in the standard 3 flavor mixing scheme; θ_{12}, θ_{13}, θ_{23}, δ, and two squared mass difference of Δm^2_{12} and Δm^2_{23}. Here solar oscillation parameters are fixed to the measured values as $\sin^2 2\theta_{12} = 0.825$ and $\Delta m^2_{12} = 8.3 \times 10^{-5}$ eV^2. Another mass difference is also fixed as $\Delta m^2_{23} = 2.5 \times 10^{-3}$ eV^2 where normal mass hierarchy ($\Delta m^2_{23} \equiv m^2_3 - m^2_2 > 0$) is assumed. Remaining 4 parameters are varied within the current experimental knowledge as;

$$\begin{aligned} s^2_{23} &= 0.40, 0.45, 0.50, 0.55, 0.60 \\ s^2_{13} &= 0.04, 0.02, 0.006, 0.00 \\ \delta &= 0^\circ, 45^\circ, 90^\circ, 135^\circ, 180^\circ, 225^\circ, 270^\circ, 315^\circ \end{aligned} \tag{3}$$

resulting in $5 \times 4 \times 8 = 160$ combinations.

These MC events are used as fake data as well as expectation. To make fake data, the MC is weighted by livetime and oscillation probabilities. Exposures of the fake data are (1) 20 years of SK (450 kton·years) or (2) 80 years of SK (1800 kton·years), which correspond to (1') 1 year of Hyper-Kamiokande (HK) or (2') 4 years of HK, respectively. Here, it is implicitly assumed that HK can achieve same detector performance as SK.

To investigate the future sensitivities, each fake data sets is compared with the 100 years of MC using Poisson statistics χ^2.

$$\begin{aligned} \chi^2 &\equiv \sum_n \left[2\left(N^n_{MC}(1 + \sum_i f^n_i \cdot \epsilon_i) - N^n_{DT} \right) + 2N^n_{DT} \ln\left(\frac{N^n_{DT}}{N^n_{MC}(1 + \sum_i f^n_i \cdot \epsilon_i)} \right) \right] \\ &+ \sum_i \left(\frac{\epsilon_i}{\sigma_i} \right)^2 \end{aligned} \tag{4}$$

where

n : suffix for event type, momentum, and zenith angle

N^n_{MC} : the number of MC events in the n-th bin

N^n_{DT} : the number of fake data events in the n-th bin

ϵ_i : systematic uncertainties (fitting parameters)

σ_i : estimated size of systematic uncertainties

f^n_i : error coefficients.

The definition of χ^2 and data binning are same as Super-Kamiokande analyses [7]. Moreover, same set of systematic uncertainties ($\epsilon_i; i = 1 \sim 44$) is used which covers uncertainties of neutrino flux, interactions, detector response, and event reconstructions [7].

Because the fake data are made from MC events, χ^2 minimum is always obtained as $\chi^2_{min} = 0$ with all $\epsilon_i = 0$ at oscillation parameters that are used in weighting the fake data. In following sections, sensitivities of each oscillation parameters are evaluated by $\Delta\chi^2 \equiv \chi^2_{min}(\text{test point}) - \chi^2_{min}(\text{true point}) = \chi^2_{min}(\text{test point})$.

4. Analyses

4.1. Octant of θ_{23}

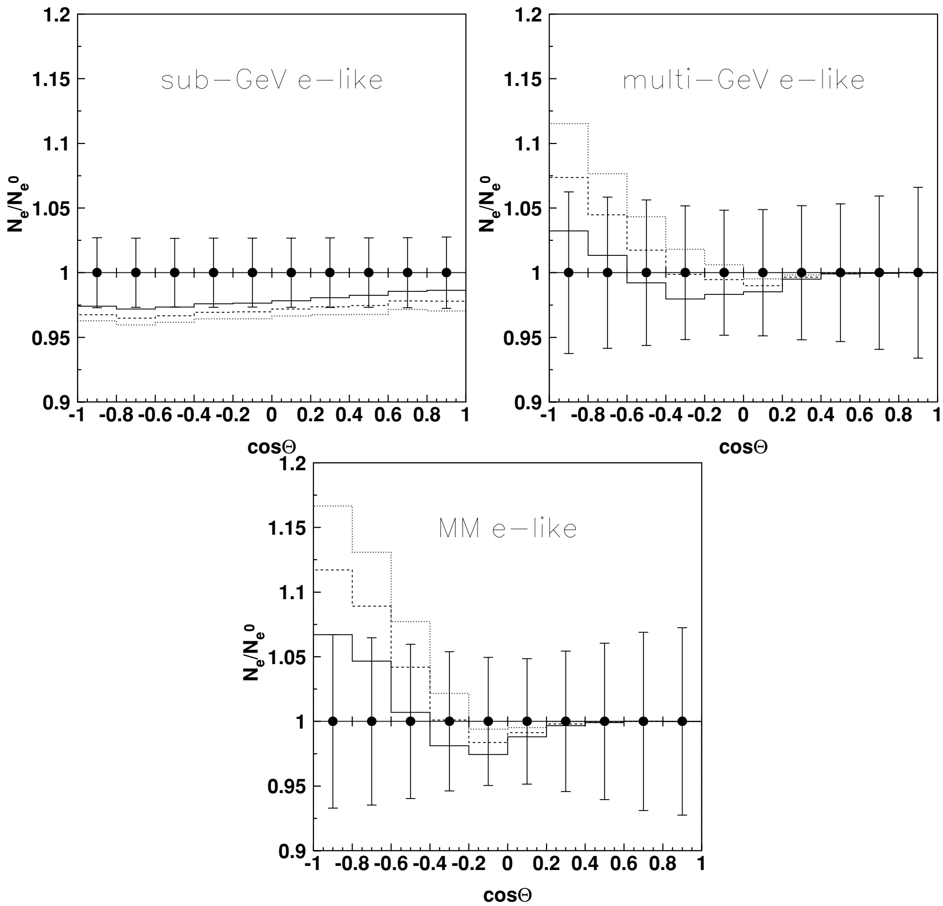

Fig 2. Expected event rate changes in sub-GeV single-ring e-like, multi-GeV single-ring e-like, and multi-GeV multi-ring e-like (labeled as MM e-like) event samples. True θ_{23} is varied as $s^2_{23} = 0.4$ (solid), $s^2_{23} = 0.5$ (dashed) , and $s^2_{23} = 0.6$ (dotted). Parameters are assumed as $(\sin^2 2\theta_{12}, s^2_{23}, s^2_{13}, \delta, \Delta m^2_{12}, \Delta m^2_{23})$ $= (0.825, 0.4 \sim 0.6, 0.04, 45°, 8.3 \times 10^{-5}\text{eV}^2, 2.5 \times 10^{-3}\text{eV}^2)$. Points with error bars represent null oscillation expectations with expected statistical errors for 20 years of SK.

Figure 2 show the event rate changes in sub-GeV single-ring e-like, multi-GeV single-ring e-like, and multi-GeV multi-ring e-like event samples for different

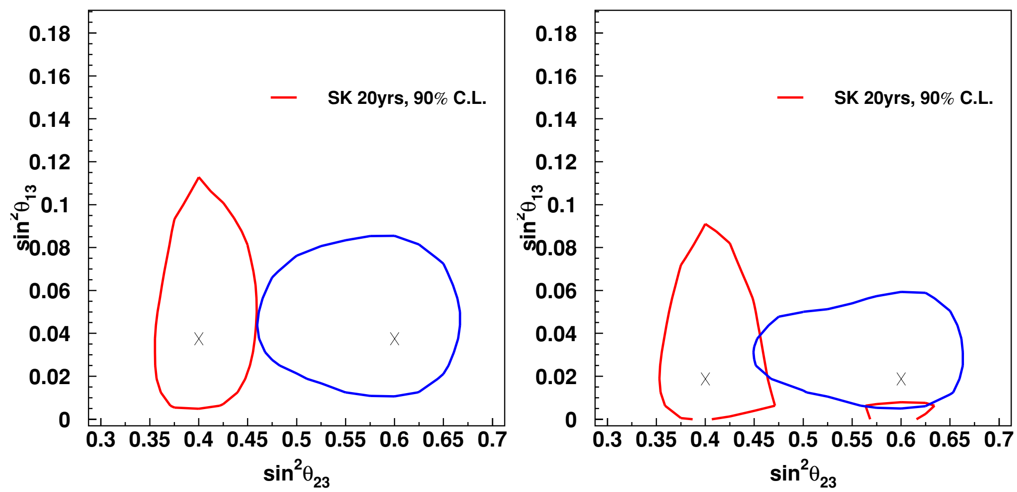

Fig 3. Expected sensitivities for s_{23}^2 and s_{13}^2 at 90% CL with livetime of 20 years of SK. Crosses in the contours represent the assumed true mixing angles. $(s_{23}^2, s_{13}^2) = (0.4 \mathrm{or} 0.6, 0.04)$ (left figure) and $(s_{23}^2, s_{13}^2) = (0.4 \mathrm{or} 0.6, 0.02)$ (right figure). We expect to discriminate between $s_{23}^2 = 0.4$ and $s_{23}^2 = 0.6$ if s_{13}^2 is larger than 0.02. Parameters are assumed as $(\sin^2 2\theta_{12}, s_{23}^2, s_{13}^2, \delta, \Delta m_{12}^2, \Delta m_{23}^2)$ $= (0.825, 0.4 \mathrm{or} 0.6, 0.02 \mathrm{or} 0.04, 45°,\ 8.3 \times 10^{-5}\mathrm{eV}^2, 2.5 \times 10^{-3}\mathrm{eV}^2)$.

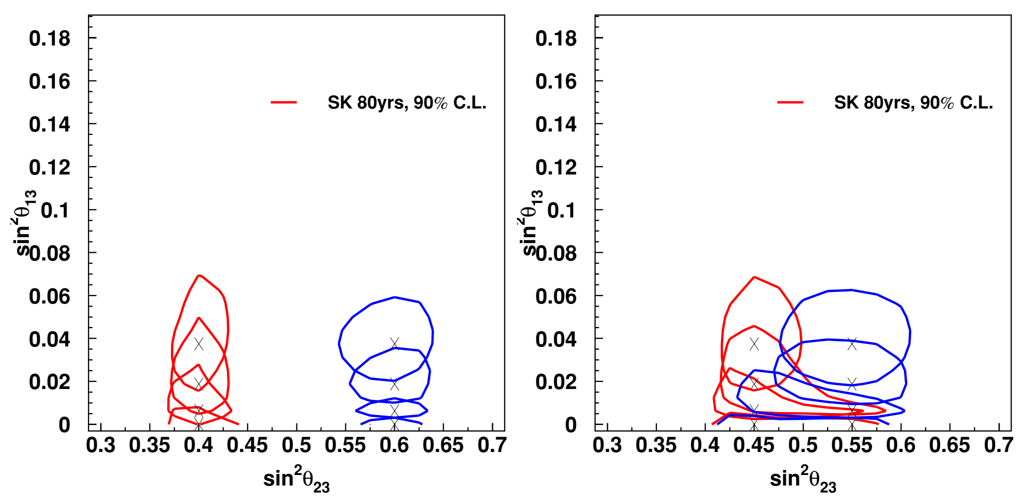

Fig 4. Expected sensitivities for s_{23}^2 and s_{13}^2 at 90% CL with livetime of 80 years of SK. Crosses in the contours represent the assumed true mixing angles. We expect to clearly discriminate between $s_{23}^2 = 0.4$ and $s_{23}^2 = 0.6$. Even discrimination between $s_{23}^2 = 0.45$ and $s_{23}^2 = 0.55$ is expected if s_{13}^2 is close to 0.04. Parameters are assumed as $(\sin^2 2\theta_{12}, s_{23}^2, s_{13}^2, \delta, \Delta m_{12}^2, \Delta m_{23}^2) = (0.825, 0.4 \sim 0.6, 0.00 \sim 0.04, 45°,$ $8.3 \times 10^{-5}\mathrm{eV}^2, 2.5 \times 10^{-3}\mathrm{eV}^2)$.

s_{23}^2 values. We expect event rate changes in sub-GeV electrons and zenith angle distortions in multi-GeV single- and multi-ring electron samples.

Figure 3 shows the expected sensitivities for s_{23}^2 and s_{13}^2 evaluated by $\Delta\chi^2$. We can expect to discriminate between $s_{23}^2 = 0.4$ and $s_{23}^2 = 0.6$ with livetime of SK 20 years if s_{13}^2 is larger than 0.02. On the other hand, discrimination between $s_{23}^2 = 0.45$ and $s_{23}^2 = 0.55$ requires more data statistics.

Figure 4 show the expected sensitivities with statistics of SK 80 years. We can expect to discriminate between $s_{23}^2 = 0.4$ and $s_{23}^2 = 0.6$ for any θ_{13}. Even discrimination between $s_{23}^2 = 0.45$ and $s_{23}^2 = 0.55$ will be possible if s_{13}^2 is close to 0.04.

4.2. θ_{13} sensitivity

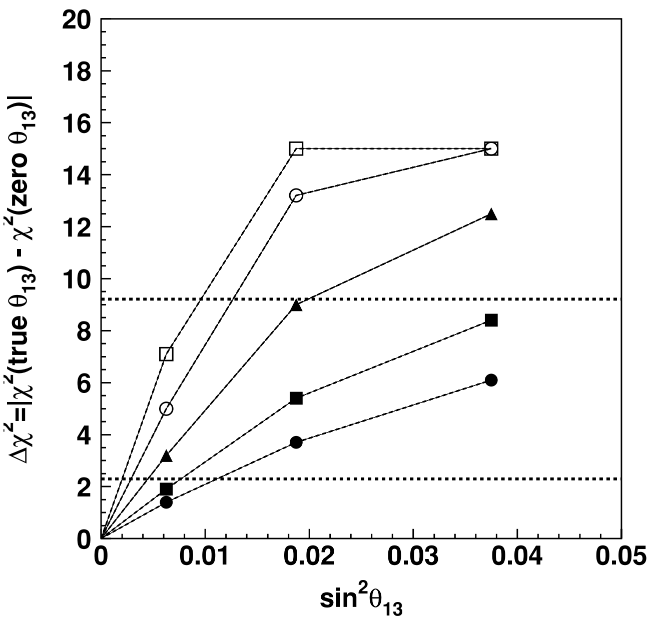

Fig 5. Significance for nonzero θ_{13} as a function of s_{13}^2 for 20 years of SK exposure. From bottom to top, $s_{23}^2 = 0.4$ (filled circle), 0.45 (filled square), 0.50 (filled triangle), 0.55 (open circle), and 0.60 (open square). 3σ significance is shown by the horizontal line at $\Delta\chi^2 = 9.2$. $\Delta\chi^2$ is found to be quadruple in the case of 80 years exposure and $\Delta\chi^2 = 9.2/4$ line is also shown to see the 3σ border for 80 years. Oscillation parameters are assumed as $(\sin^2 2\theta_{12}, s_{23}^2, s_{13}^2, \delta, \Delta m_{12}^2, \Delta m_{23}^2)$ $= (0.825, 0.4 \sim 0.6, 0.00 \sim 0.04, 45°,\ 8.3 \times 10^{-5}\text{eV}^2, 2.5 \times 10^{-3}\text{eV}^2)$.

Figure 3 and Figure 4 in the previous section also show the sensitivity for θ_{13} measurements. It is seen that zero θ_{13} is excluded in the case that true θ_{13} is relatively large. We can evaluate the power to exclude non-zero θ_{13} by calculating the difference between χ_{min}^2 at $\theta_{13} = 0$ and χ_{min}^2 at $\theta_{13} =$ true θ_{13}.

Figure 5 shows the χ^2 difference for each s_{23}^2 as a function of s_{13}^2. For larger s_{23}^2, the significance gets larger thanks to the θ_{13} resonance (the third term in Equation 2). By the livetime of SK 20 years, we expect more than 3σ significance in the case that θ_{23} is in the second octant and s_{13}^2 is larger than 0.02. The sensitivity can be improved by increasing data statistics and 3σ discrimination will be possible for all θ_{23} if s_{13}^2 is larger than 0.01.

4.3. CP phase

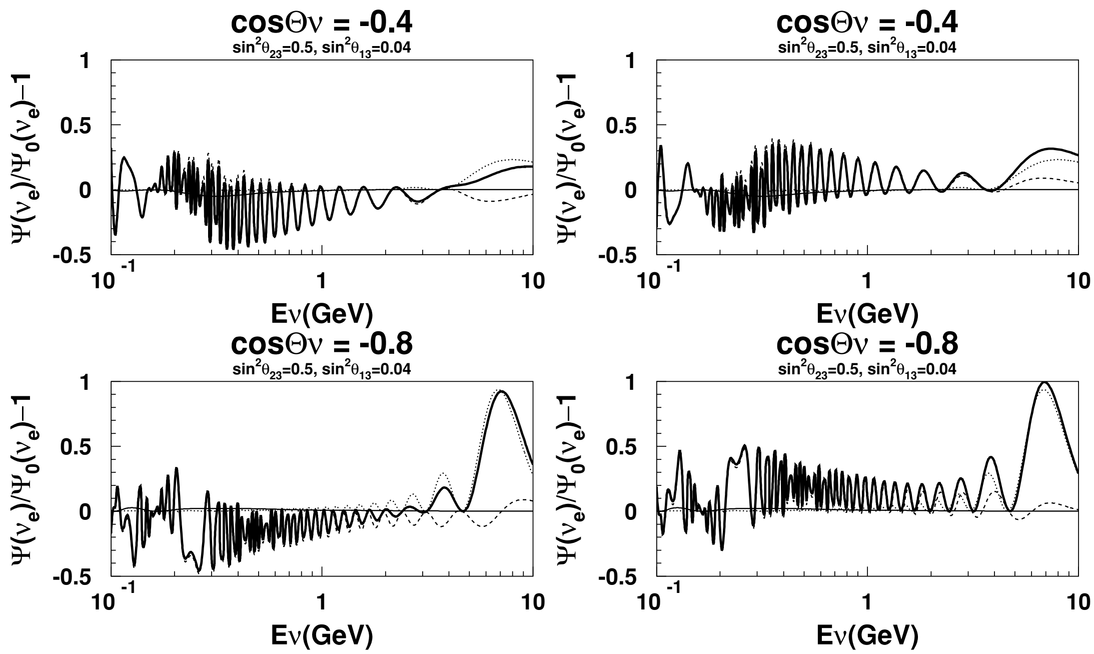

Fig 6. Oscillated ν_e flux relative to the non-oscillated flux as a function of neutrino energy. $\delta = 45°$ (left figures) and $\delta = 225°$ (right figures) and neutrino direction of $\cos\Theta_\nu = -0.4$ (upper figures) and $\cos\Theta_\nu = -0.8$ (bottom figures). Parameters are assumed as $(\sin^2 2\theta_{12}, s_{23}^2, s_{13}^2, \delta, \Delta m_{12}^2, \Delta m_{23}^2) = (0.825, 0.5, 0.04, 45°\text{or}225°, 8.3 \times 10^{-5}\text{eV}^2, 2.5 \times 10^{-3}\text{eV}^2)$. Thin solid lines, dashed lines, and dotted lines correspond to Δm_{12}^2 term, interference term, and resonance term, respectively (see Equation 2). Thick solid lines are total fluxes.

The effect of CP phase δ expressed by the second term in Equation 2 can be seen in the neutrino energy region of 100MeV$\sim$10GeV. Figure 6 shows calculated ν_e flux for $\delta = 45°$ and $\delta = 225°$. The flux distributions are steep against neutrino energy as well as zenith angle of neutrino direction. These distributions are smeared by neutrino interactions and event reconstructions.

Figure 7 shows expected event rate changes in each observed event types

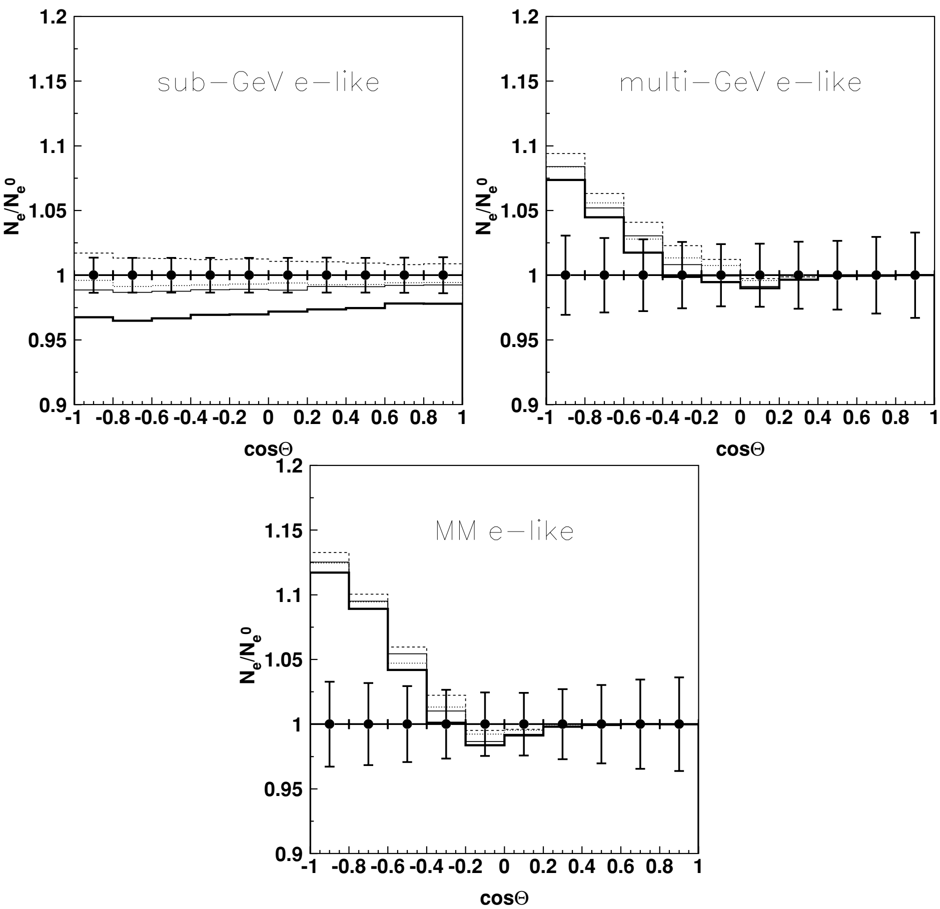

Fig 7. Expected event rate changes in sub-GeV single-ring e-like, multi-GeV single-ring e-like, and multi-GeV multi-ring e-like event samples. True CP phase δ is varied as 45° (thick solid), 135° (thin solid), 225° (thin dashed), and 315° (thin dotted). True parameters are assumed as $(\sin^2 2\theta_{12}, s_{23}^2, s_{13}^2, \delta, \Delta m_{12}^2, \Delta m_{23}^2)$ $= (0.825, 0.5, 0.04, 0° \sim 360°$, $8.3 \times 10^{-5}\mathrm{eV}^2, 2.5 \times 10^{-3}\mathrm{eV}^2)$. Points with error bars represent null oscillation expectation with expected statistical errors for 80 years of SK.

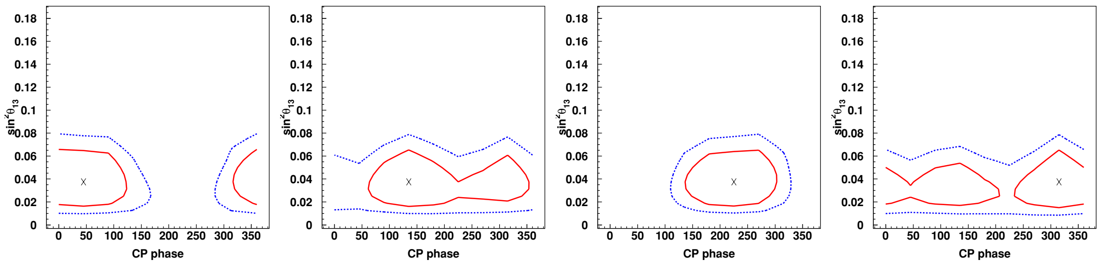

Fig 8. Expected sensitivities for δ and s_{13}^2 at 90% CL (solid) and 99% CL (dashed) with livetime of SK 80 years. Crosses in the contours represent the true parameters. We assumed $(\sin^2 2\theta_{12}, s_{23}^2, s_{13}^2, \delta, \Delta m_{12}^2, \Delta m_{23}^2) = (0.825, 0.5, 0.04, 0° \sim 360°, 8.3 \times 10^{-5}\text{eV}^2, 2.5 \times 10^{-3}\text{eV}^2)$.

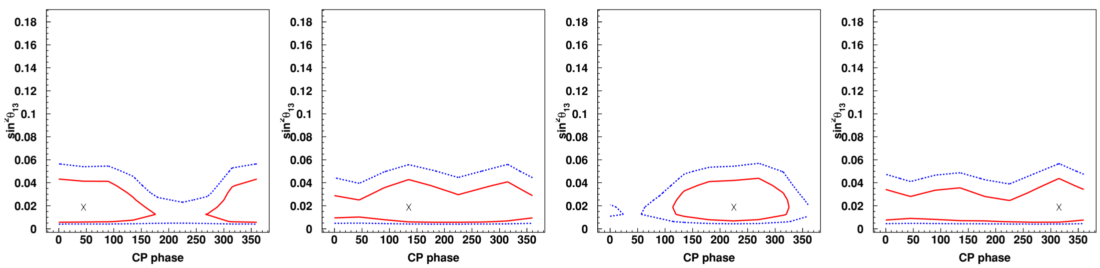

Fig 9. Expected sensitivities for δ and s_{13}^2 at 90% CL (solid) and 99% CL (dashed) with livetime of SK 80 years. Crosses in the contours represent the true parameters. We assumed $(\sin^2 2\theta_{12}, s_{23}^2, s_{13}^2, \delta, \Delta m_{12}^2, \Delta m_{23}^2) = (0.825, 0.5, 0.02, 0° \sim 360°, 8.3 \times 10^{-5}\text{eV}^2, 2.5 \times 10^{-3}\text{eV}^2)$.

for different δ values. The size of the CP effect is $1 \sim 3\%$ and it is comparable with or even smaller than the size of statistical errors for 80 years of SK.

Figure 8 and Figure 9 show the expected sensitivity for CP phase evaluated by $\Delta\chi^2$. In the case of $s_{13}^2 = 0.04$ (Figure 8), measurement of CP phase for $\delta = 45°$, 135°, 225°, and 315° is expected to be possible by 90% CL and even 99% CL measurement is expected for $\delta = 45°$ and 225°. In the case of $s_{13}^2 = 0.02$ (Figure 9), accuracy of CP phase measurements gets worse but some constraints could be obtained in some cases. These sensitivities don't depend on θ_{23} much and true $s_{23}^2 = 0.5$ is assumed in these figures.

5. Conclusion

By using detailed simulation of neutrino interactions, detector simulation, and event reconstructions, future sensitivities for neutrino mixing angles and CP phase by atmospheric neutrino experiments have been studied. Here, it is assumed that θ_{12}, Δm^2_{12}, and Δm^2_{23} will be measured with high accuracy by other experiments and these parameters are fixed in this study.

The effect of each parameters, θ_{23}, θ_{13}, and δ, on e-like events have been calculated and shown in this article. Then sensitivities for oscillation parameters were evaluated by χ^2 fitting taking into account detailed systematic uncertainties.

We expect to discriminate between $s^2_{23} = 0.4$ and 0.6 with livetime of SK 20 years if s^2_{13} is larger than 0.02. With statistics of SK 80 years, we expect to discriminate between $s^2_{23} = 0.4$ and 0.6 for any θ_{13} and even discrimination between $s^2_{23} = 0.45$ and 0.55 will be possible if s^2_{13} is close to 0.04. As for nonzero θ_{13}, we expect more than 3σ significance in the case of $(\theta_{23} > \pi/4, s^2_{13} > 0.02)$ with 20 years SK and in the case of $(s^2_{13} > 0.01)$ with 80 years SK. Finally, there is a chance to measure CP phase with 80 years SK statistics if $s^2_{13} > 0.02$. In general, if θ_{13} is close to the CHOOZ limit, future atmospheric neutrino observation could give us precious information on θ_{23}, θ_{13}, and even δ.

It appears that the size of oscillation effect is relatively small, especially in CP measurement. Therefore, it is really indispensable to well understand neutrino fluxes, interactions, and detector response in future neutrino oscillation studies.

6. Acknowledgment

The authors thank to the workshop organizers and participants for the exciting workshop. It was really good opportunity for experts of neutrino flux, interactions, neutrino oscillations, and observations to get together and discuss the future possibilities of atmospheric neutrinos.

References

[1] Super-Kamiokande collaboration, Phys. Rev. Lett. 81 (1998) 1562; Super-Kamiokande collaboration, Phys. Rev. Lett. 93 (2004) 101801.
[2] Super-Kamiokande collaboration, hep-ex/0501064.
[3] Super-Kamiokande collaboration, Phys. Rev. D68 (2003) 092002; Super-Kamiokande collaboration, Phys. Rev. D69 (2004) 011104; SNO collaboration, Phys. Rev. Lett. 87 (2001) 071301;. KamLAND collaboration, Phys. Rev. Lett. 94 (2005) 081801.
[4] CHOOZ collaboration, Phys. Lett. B466 (1999) 415-430.
[5] for example Concha Conzalez-Garcia, talk in the workshop; E. Lici, talk in the workshop.
[6] O. L. G. Pares and A. Yu. Smirnov, hep-ph/0309312.
[7] K. Okumura, talk in the workshop; K. Okumura, Ph.D. thesis (1999) Univ. of Tokyo.